

Supporting Information

Formation of cobalt phosphide nanodisks as a bifunctional electrocatalyst for enhanced water splitting

*Lvlv Ji, *^a Huifang Zheng,^a Yue Wei,^a Yeting Fang,^a Jialei Du,^b Tao Wang^a and Sheng Wang*^a*

^a School of Materials Science and Engineering, Zhejiang Sci-Tech University, Hangzhou 310018, China

^b Institute for Advanced Interdisciplinary Research, University of Jinan, Jinan 250022, China

*Corresponding author, E-mail: llji@zstu.edu.cn; wangsheng571@hotmail.com

EXPERIMENTAL

Materials. Cobalt chloride (99.9%), potassium hexacyanocobaltate(III) (99%), ammonia solution (AR, 28~30%), sodium hypophosphite (99%), potassium hydroxide (99.999%) and RuO₂ (99.9%) were purchased from MACKLIN Reagent Co. 20 wt% Pt/C was purchased from Alfa Aesar Chemical Reagent Co. High-purity argon gas (99.999%) was purchased from Shanghai Gases Co. All other chemical reagents were of analytical grade and used as received without further purification. All electrolyte solutions were prepared by Milli-Q ultrapure water (> 18 MΩ).

Apparatuses. Scanning electron microscopy (SEM) images and energy dispersive X-ray analysis (EDX) data were obtained at Hitachi S-4800 (Hitachi, Japan) equipped with a Horiba EDX system (X-max, silicon drift X-Ray detector). SEM images were obtained with an acceleration voltage of 5 kV and EDX spectrum was obtained with an acceleration voltage of 15 kV. Transmission electron microscopy (TEM) images, high-resolution TEM (HRTEM) images and selected area electron diffraction (SAED) patterns were obtained at JEM-2100, JEOL.

Powder X-ray diffraction (XRD) was conducted by Bruker Focus D8 *via* ceramic monochromatized Cu K α radiation of 1.54178 Å, operating at 40 kV and 40 mA. FT-IR spectra were measured on a Nicolet 6700 spectrometer (Thermo Fisher Nicolet, USA) with KBr pellets. Raman spectra were measured on a confocal microscope laser Raman spectrometer (Rainshaw invia). The Brunauer-Emmett-Teller (BET) specific surface areas of the samples were measured on a TRISTAR 3020 by nitrogen adsorption at 77.4 K.

X-ray photoelectron spectroscopy (XPS) for elemental analysis was measured on a Kratos Axis Ultra DLD X-ray Photoelectron Spectrometer using 100 W monochromated Al K α radiation as the X-ray source for excitation. The 500 μ m X-ray spot was used for XPS analysis. The base pressure in the analysis chamber was about 3×10^{-10} mbar. The C 1s peak (284.6 eV) was used for internal calibration.

Electrochemical measurements were conducted on a CHI 660E electrochemical workstation (Chenhua Corp., Shanghai, China).

Synthesis of Co-Co PBA NCs. The synthesis of Co₃[Co(CN)₆]₂ nanocubes (Co-Co PBA NCs) follows a precipitation method. Briefly, cobalt chloride (0.6 mmol) and sodium citrate (0.9 mmol) were firstly dissolved in 20 ml H₂O to form solution A, and potassium hexacyanocobaltate(III) (0.4 mmol) was dissolved in 20 ml H₂O to form solution B. Then, the solution A and solution B were mixed by magnetic stirring for 3 min. After that, the reaction was carried out at 3 – 5 °C undisturbed for 24 h. The product was collected by filtration and washed with deionized water and ethanol for several times. The obtained pink powder Co-Co PBA NCs was dried in a vacuum oven at 60 °C for 24 h.

Synthesis of Co-Co PBA NDs, Co-Co PBA ET-2 and Co-Co PBA ET-4. In the typical synthesis procedure, 6 ml ammonia solution (28~30%) was mixed with 15 ml H₂O to form solution A, and Co-Co PBA NCs (20 mg) was dispersed in 10 ml ethanol to form solution B. Then, the solution A and solution B was mixed and stirred for 10 min at room temperature. The etched powder sample was collected by filtration and washed with abundant deionized water until the pH of filtrate reaching 7. The obtained

Co-Co PBA NDs was dried in a vacuum oven at 60 °C for 24 h. In the parallel experiments, the Co-Co PBA ET-2 and Co-Co PBA ET-4 samples were prepared under identical conditions except that the added ammonia solution volume in solution A was 2 and 4 ml, respectively.

Synthesis of CoP NDs, CoP NCs, CoP ET-2 and CoP ET-4. In the typical synthesis procedure, Co-Co PBA NDs (20 mg) and NaH₂PO₂ (200 mg) were placed at two separate positions in a porcelain boat with NaH₂PO₂ powder at the upstream side of the tube furnace. The samples were annealed under an argon atmosphere at 300 °C for 2 h with a ramping rate of 2 °C min⁻¹. In the parallel experiments, the CoP NCs, CoP ET-2 and CoP ET-4 samples were prepared under identical conditions except that the precursors were Co-Co PBA NCs, Co-Co PBA ET-2 and Co-Co PBA ET-4, respectively.

Electrochemical measurements. To prepare the working electrode, the electrocatalyst (4 mg) and 5 wt% Nafion solution (80 μl) were dispersed in 1 ml of 4:1 (v/v) water/ethanol. Then, the electrocatalyst suspension (5 μl) were dropped onto a glassy carbon electrode (mass loading ~ 0.265 mg cm⁻²), which was dried as working electrode. The three-electrode system consisted of a working electrode, a carbon rod counter electrode, and a saturated calomel reference electrode (SCE). The glass cell and Teflon cell were used for the electrochemical measurements in acidic and alkaline electrolyte, respectively. The potentials reported were referred to the Reversible Hydrogen Electrode (RHE) *via* the Nernst equation: $E_{\text{RHE}} = E_{\text{SCE}} + 0.059\text{pH} + 0.244$. In 0.5 M H₂SO₄, $E_{\text{RHE}} = 0.273 \text{ V} + E_{\text{SCE}}$; in 1 M KOH, $E_{\text{RHE}} = 1.05 \text{ V} + E_{\text{SCE}}$. The HER

catalytic performance was examined in N₂-saturated 0.5 M H₂SO₄ and 1 M KOH, respectively, whereas the OER catalytic performance was evaluated in O₂-saturated 1 M KOH. Unless stated otherwise, linear sweep voltammetry (LSV) was measured at a scan rate of 2 mV s⁻¹. The Tafel slope was obtained from the LSV plot using a linear fit applied to points in the Tafel region. Electrochemical impedance spectroscopy (EIS) measurements were conducted from 10⁻² Hz to 10⁶ Hz with amplitude of 5 mV at different potentials. The electrochemical catalytic stability of the electrocatalyst was carried out by continuous cyclic voltammetry (CV) scanning and long-term electrolysis. The electrochemical double-layer capacitance (C_{dl}) of the electrocatalyst was determined by CV measurements under the potential range of 0.1 – 0.3 V vs. RHE with various scan rates in 0.5 M H₂SO₄. The resulting current density between the anodic and cathodic sweep at 0.2 V vs. RHE shows a linear dependence on the scan rate. C_{dl} can be evaluated from the slope of the linear plot. Unless stated otherwise, LSV and Tafel data plots were corrected with 90% *iR* compensation. The experiments were all performed at 22 ± 2 °C.

KOH Electrolyte Purification. In order to avoid the possible Fe contamination, the 1 M KOH electrolyte was purified according to the reported method (*J. Am. Chem. Soc.* **2015**, *137*, 3638). Firstly, Co(OH)₂ was prepared by the precipitation reaction between Co(NO₃)₂ (99.999%) and 0.1 M KOH (KOH, 99.999%) and washed three times with ultrapure water. Co(OH)₂ was then added into 1 M KOH electrolyte and stirred for 10 min to absorb the possible Fe impurities. The resultant 1 M Fe-free KOH electrolyte (supernatant) was obtained by centrifugation and used for electrochemical

measurements.

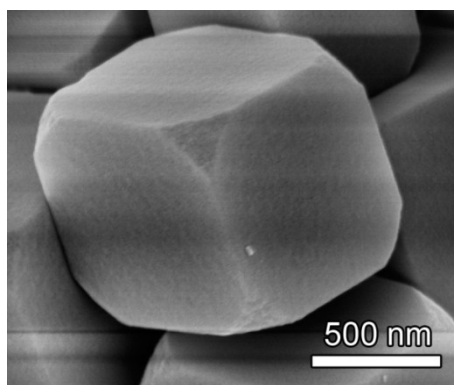


Figure S1. Enlarged SEM image of Co-Co PBA NCs with obtuse corners.

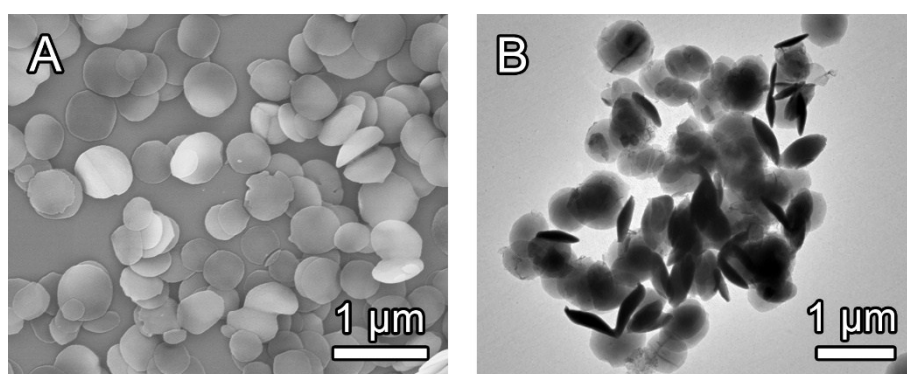


Figure S2. Large-area (A) SEM and (B) TEM image of Co-Co PBA NDs.

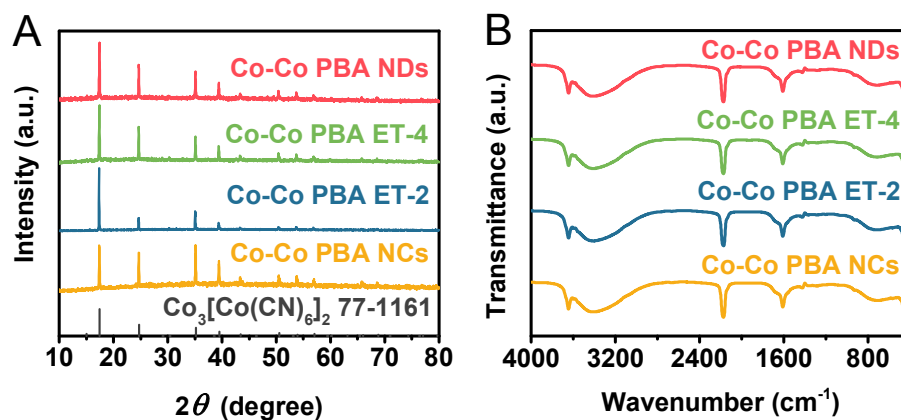


Figure S3. (A) XRD patterns and (B) FT-IR spectra of Co-Co PBA NCs, Co-Co PBA ET-2, Co-Co PBA ET-4 and Co-Co PBA NDs.

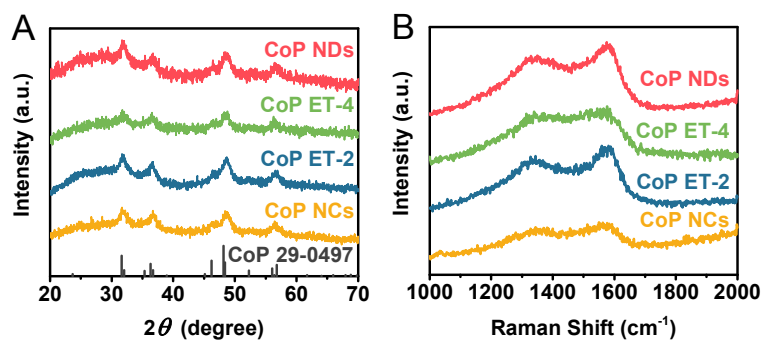


Figure S4. (A) XRD patterns and (B) Raman spectra of CoP NCs, CoP ET-2, CoP ET-4 and CoP NDs. The I_d/I_g peak intensity ratios obtained for CoP NCs, CoP ET-2, CoP ET-4 and CoP NDs are 0.82, 0.8, 0.83 and 0.79, respectively.

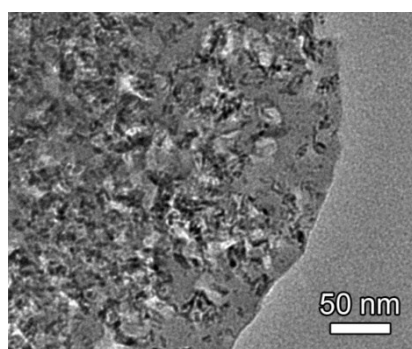


Figure S5. Enlarged TEM image of CoP NDs with numerous small pores.

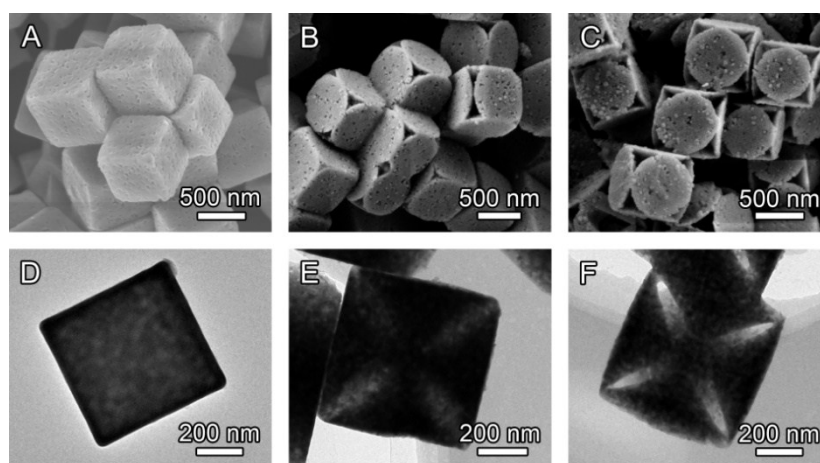


Figure S6. (A, B, C) SEM images and (D, E, F) TEM images of CoP NCs, CoP ET-2, CoP ET-4, respectively.

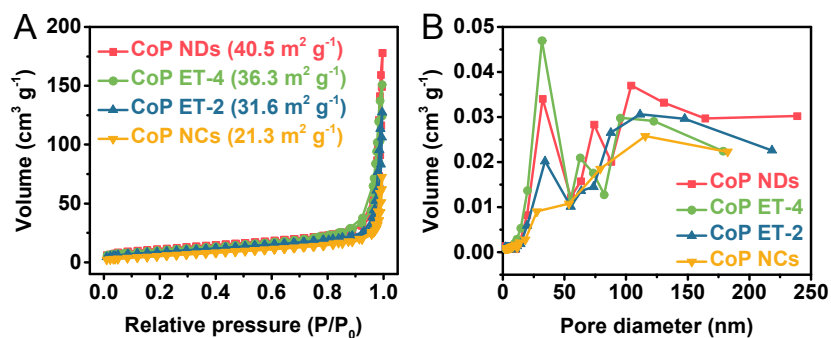


Figure S7. (A) N_2 adsorption/desorption isotherms and (B) pore size distribution plots of CoP NCs, CoP ET-2, CoP ET-4 and CoP NDs.

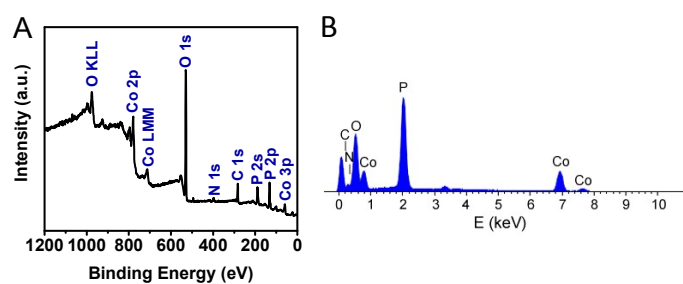


Figure S8. (A) XPS survey spectrum and (B) EDX spectrum of CoP NDs.

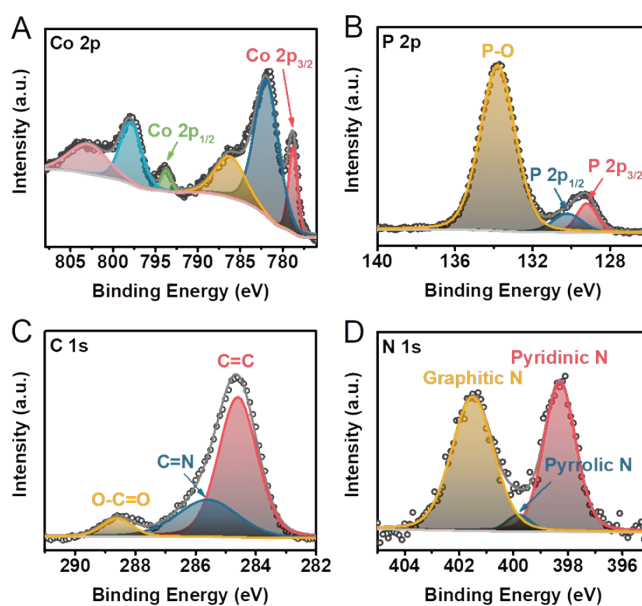


Figure S9. High-resolution XPS spectra of (A) Co 2p, (B) P 2p, (C) C 1s and (D) N 1s of CoP NDs.

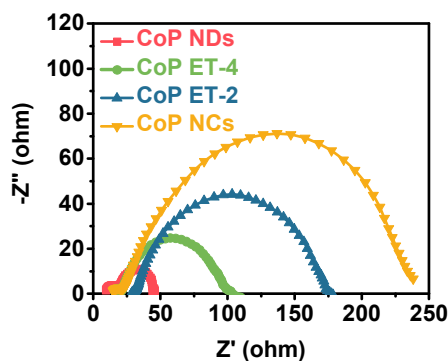


Figure S10. Nyquist plots of CoP NCs, CoP ET-2, CoP ET-4 and CoP NDs in 0.5 M H_2SO_4 under an overpotential of 150 mV for HER.

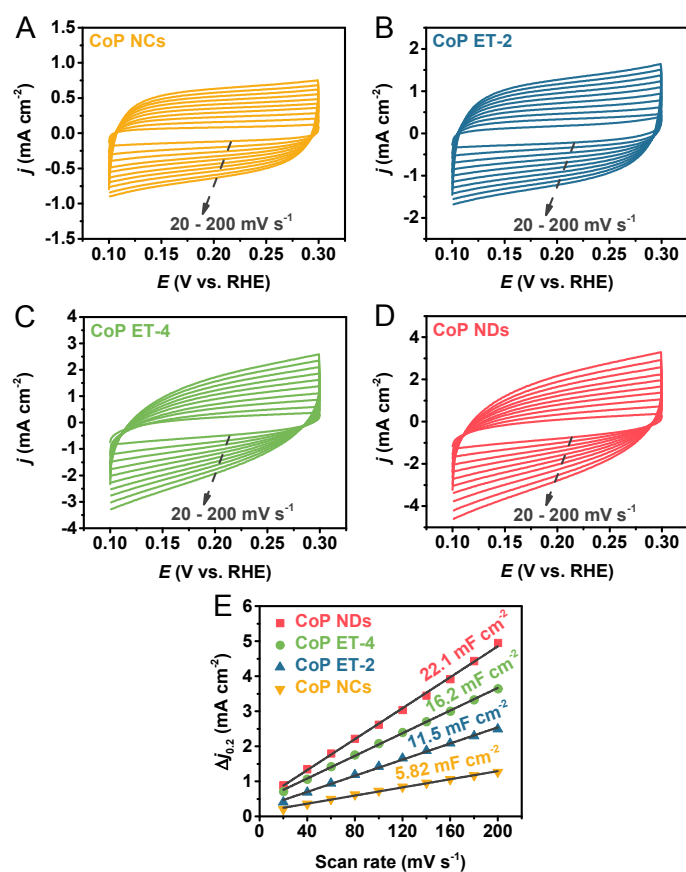


Figure S11. CVs of (A) CoP NCs, (B) CoP ET-2, (C) CoP ET-4 and (D) CoP NDs at different scan rates from 20 to 200 mV s^{-1} under the potential window of 0.1 - 0.3 V vs. RHE in 0.5 M H_2SO_4 . (E) The capacitive current at 0.2 V as a function of scan rate for CoP NCs, CoP ET-2, CoP ET-4 and CoP NDs.

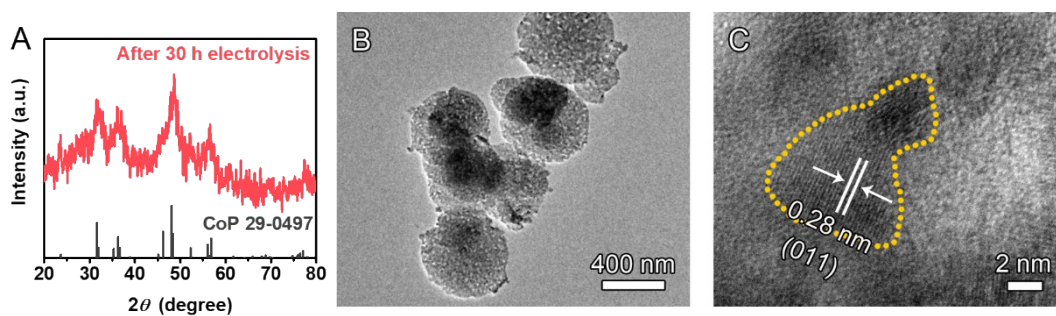


Figure S12. (A) XRD pattern, (B) TEM image and (C) HRTEM image of CoP NDs after 30 h electrolysis in 0.5 M H₂SO₄.

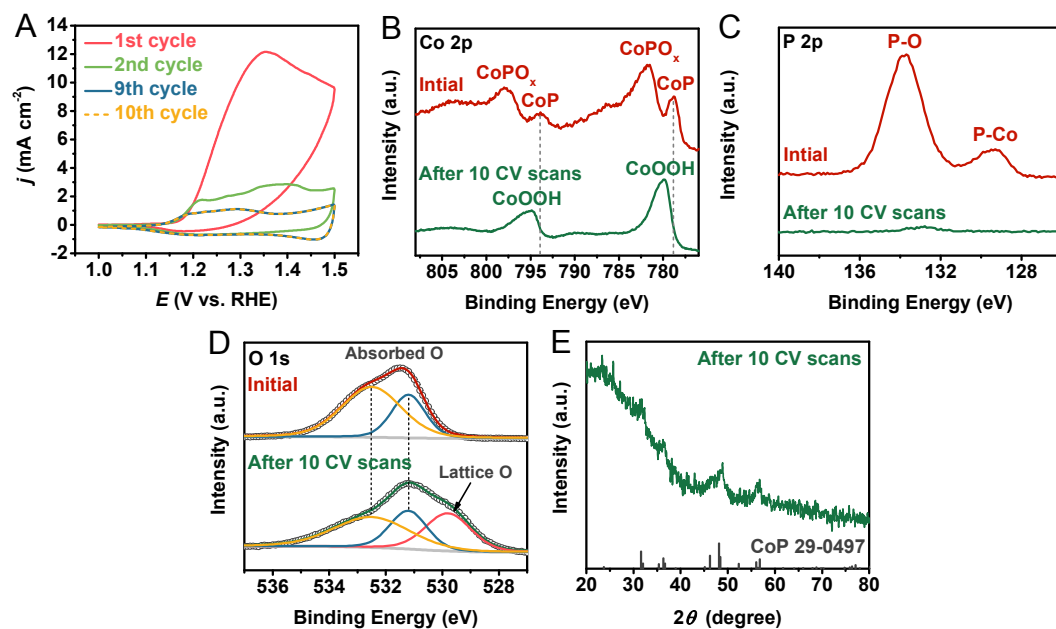


Figure S13. (A) The first, second, 9th and 10th CV scan of CoP NDs in 1 M KOH under the potential range of 1 – 1.5 V vs. RHE at 2 mV s⁻¹. High-resolution (B) Co 2p, (C) P 2p and (D) O 1s XPS spectra of the as-prepared CoP NDs and CoP NDs after 10 CV scans. (E) XRD pattern of CoP NDs after 10 CV scans.

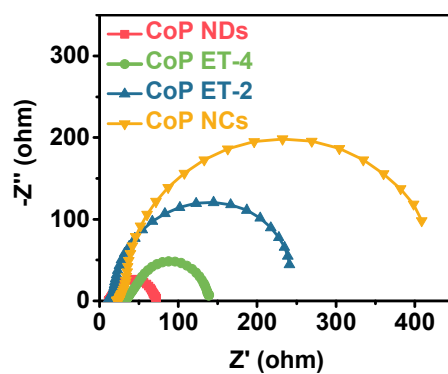


Figure S14. Nyquist plots of CoP NCs, CoP ET-2, CoP ET-4 and CoP NDs in 1 M KOH under an overpotential of 340 mV for OER.

Table S1. Comparison of HER activity of CoP NDs with recently reported noble-metal-free electrocatalysts in 0.5 M H₂SO₄.

Electrocatalyst	Loading mass (mg cm ⁻²)	Substrate	η_{10} (mV)	b (mV dec ⁻¹)	Ref.
CoP NDs	0.265	GCE^{a)}	126	54.5	This work
CoP@NG	0.283	GCE	158	63.8	<i>Electrochim. Acta</i> 2019 , 307, 543
CoP/Co ₂ P@NC-2	-	GCE	126	79	<i>ACS Sustainable Chem. Eng.</i> 2019 , 7, 8993
CoP/NCNHP	-	GCE	140	53	<i>J. Am. Chem. Soc.</i> 2018 , 140, 2610
PANI/CoP HNWs	0.8	CC ^{b)}	57	34.5	<i>J. Am. Chem. Soc.</i> 2018 , 140, 5118
CoP-CNTs	-	GCE	139	52	<i>Small</i> 2017 , 13, 1602873
α -MoC _{1-x} /NC	-	GCE	142	74	<i>ACS Sustainable Chem. Eng.</i> 2019 , 7, 9637
NP-doped holey graphene	3	GCE	344	118	<i>Adv. Sci.</i> 2019 , 6, 1900119
NbS ₂ /CP	0.285	CP ^{c)}	90	125	<i>ACS Appl. Mater. Interfaces</i> 2019 , 11, 13205
FNC-MoS ₂	0.535	GCE	194	54	<i>Carbon</i> 2019 , 150, 363
Co ₉ S ₈ @NOSC-900	0.28	GCE	235	72	<i>Adv. Funct. Mater.</i> 2017 , 27, 1606585
3D-Co(16.4%)-MoS ₂ /G	0.5	GCE	143	71	<i>Nano Energy</i> 2019 , 61, 611
CE-TaS ₂	0.285	GCE	192	66	<i>CrystEngComm</i> 2019 , 21, 3517
Zn _{1/3} Co _{2/3} MoS ₃ microboxes	-	GCE	160	85	<i>ACS Sustainable Chem. Eng.</i> 2019 , 7, 9800
W-W ₂ C/CNT-6	0.28	GCE	155	56	<i>ACS Sustainable Chem. Eng.</i> 2019 , 7, 10016
FeP/CN	1	GCE	104	63.5	<i>Carbon</i> 2019 , 144, 764
B12/G800A	1.27	GCE	115	65	<i>J. Mater. Chem. A</i> 2019 , 7, 7179
Fe doped NiS ₂	-	GCE	198	42	<i>J. Mater. Chem. A</i> 2019 , 7, 4971
Ni@NC@MoS ₂	0.28	GCE	82	47.5	<i>Small</i> 2019 , 15, 1804545
FePSe ₃ /NC	0.212	GCE	70	53	<i>Nano Energy</i> 2019 , 57, 222
Ni ₂ P@NPCNFs	-	CC	63.2	56.7	<i>Angew. Chem. Int. Ed.</i> 2018 , 57, 1963
N,P-Mo _x C NF	0.265	GCE	107	65.1	<i>ACS Appl. Mater. Interfaces</i> 2018 , 10, 14632
N-Doped α -MoS _x	-	GCE	143	57	<i>Nanoscale</i> 2019 , 11, 11217
Mo ₂ N-Mo ₂ C/HGr-3	0.337	GCE	157	55	<i>Adv. Mater.</i> 2018 , 30, 1704156

^{a)}GCE represents glassy carbon electrode; ^{b)}CC represents carbon cloth; ^{c)}CP represents carbon paper.

Table S2. Comparison of HER activity of CoP NDs with recently reported noble-metal-free electrocatalysts in 1 M KOH.

Electrocatalyst	Loading mass (mg cm ⁻²)	Substrate	η_{10} (mV)	b (mV dec ⁻¹)	Ref.
CoP NDs	0.265	GCE	134	56.9	This work
CoP@NG	0.283	GCE	182	59.6	<i>Electrochim. Acta</i> 2019 , 307, 543
CoP/Co ₂ P@NC-2	-	GCE	198	82	<i>ACS Sustainable Chem. Eng.</i> 2019 , 7, 8993
CoNiP microspheres	-	GCE	145.8	52	<i>J. Mater. Chem. A</i> 2019 , 7, 8602
CoTeNR/NF	1.3	Ni foam	202	115	<i>Small Methods</i> 2019 , 1900113
CoP/NCNHP	-	GCE	115	66	<i>J. Am. Chem. Soc.</i> 2018 , 140, 2610
EG/H-Co _{0.85} Se P	2.1	Graphite foil	150	83	<i>Adv. Mater.</i> 2017 , 29, 1701589
Co-Fe oxyphosphide	-	GCE	180	62	<i>Adv. Sci.</i> 2019 , 1900576
Co ₃ O ₄ /MoS ₂	2	Ni foam	205	98	<i>Appl. Catal. B-Environ.</i> 2019 , 248, 202
NOPHC _x -900	0.28	GCE	290	102	<i>Appl. Catal. B-Environ.</i> 2019 , 248, 239
W-W ₂ C/CNT-6	0.28	GCE	147	51	<i>ACS Sustainable Chem. Eng.</i> 2019 , 7, 10016
Mo ₂ N-Mo ₂ C/HGr-3	0.337	GCE	154	68	<i>Adv. Mater.</i> 2018 , 30, 1704156
Co ₉ S ₈ @NOSC-900	0.28	GCE	320	105	<i>Adv. Funct. Mater.</i> 2017 , 27, 1606585
B12/G800A	1.27	GCE	130	77	<i>J. Mater. Chem. A</i> 2019 , 7, 7179
FePSe ₃ /NC	0.212	GCE	118.5	88	<i>Nano Energy</i> 2019 , 57, 222
Cu-Ni nanocages	-	GCE	140	79	<i>ACS Catal.</i> 2019 , 9, 5084
α -MoC _{1-x} /NC	-	GCE	118	84	<i>ACS Sustainable Chem. Eng.</i> 2019 , 7, 9637
CoCuP foam	-	Steel foil	138	48	<i>ACS Sustainable Chem. Eng.</i> 2019 , 7, 10734
3D-NiCoP		Ni foam	105	79	<i>Nano Res.</i> 2019 , 12, 375
Co-Fe-P nanotubes	0.285	GCE	86	59	<i>Nano Energy</i> 2019 , 56, 225
(Fe _{0.048} Ni _{0.952}) ₂ P	1	Ni foam	103	76.6	<i>Nano Energy</i> 2019 , 56, 813
Co ₄ Ni ₁ P NTs	0.19	GCE	129	52	<i>Adv. Funct. Mater.</i> 2017 , 27, 1703455
Cu _{0.3} Co _{0.27} P/NC	0.4	GCE	220	122	<i>Adv. Energy Mater.</i> 2017 , 7, 1601555
VOOH nanospheres	0.8	Ni foam	164	104	<i>Angew. Chem. Int. Ed.</i> 2017 , 56, 573

Table S3. Comparison of OER activity of CoP NDs with recently reported noble-metal-free electrocatalysts in 1 M KOH.

Electrocatalyst	Loading mass (mg cm ⁻²)	Substrate	η_{10} (mV)	b (mV dec ⁻¹)	Ref.
CoP NDs	0.265	GCE	318	49.1	This work
CoP@NG	0.283	GCE	354	63.8	<i>Electrochim. Acta</i> 2019 , 307, 543
Fe ₃ C@Fe,N,S-GCM	0.32	GCE	327	253.8	<i>Carbon</i> 2019 , 150, 93
CoNiS/PCNs	-	GCE	320	86	<i>Carbon</i> 2019 , 149, 144
CoNi-P-3DHFLM	0.127	GCE	292	84	<i>Appl. Catal. B-Environ.</i> 2019 , 249, 147
r-CoFe	0.212	GCE	253	39	<i>J. Mater. Chem. A</i> 2019 , 7, 14011
CoO _x -BPQDs	-	GCE	360	58.5	<i>J. Mater. Chem. A</i> 2019 , 7, 12974
Geobacter/rGO	0.05	GCE	270	43	<i>Chem. Mater.</i> 2019 , 31, 3686
Mn-doped Co ₃ O ₄ nanoflakes	0.65	Ni foam	263	60	<i>ACS Sustainable Chem. Eng.</i> 2019 , 7, 9690
Co ₃ O ₄ @BP	-	GCE	400	63	<i>ACS Appl. Mater. Interfaces</i> 2019 , 11, 17459
NSFLGDY-900	0.8	GCE	299	62	<i>J. Am. Chem. Soc.</i> 2019 , 141, 7240
Fe@BIF-91	0.23	GCE	351	71	<i>Adv. Sci.</i> 2019 , 6, 1801920
Co-P@NC-800	0.283	GCE	370	79	<i>ACS Appl. Mater. Interfaces</i> 2017 , 9, 40171
CoP/NCNHP	-	GCE	310	70	<i>J. Am. Chem. Soc.</i> 2018 , 140, 2610
CoMnO-600	-	GCE	337	82	<i>Small</i> 2017 , 13, 1700468
NiCoP/C nanoboxes	-	GCE	330	96	<i>Angew. Chem. Int. Ed.</i> 2017 , 129, 3955
Co-C ₃ N ₄ /CNT	-	GCE	380	68.4	<i>J. Am. Chem. Soc.</i> 2017 , 139, 3336
CoTe ₂ @NCNTFs	0.285	GCE	330	82.8	<i>J. Mater. Chem. A</i> 2018 , 6, 3684
G-Ni ₄ Fe/GF	0.05	Graphite foil	310	50	<i>Adv. Energy Mater.</i> 2018 , 1800403
Mo ₂ C@CS	0.4	GCE	380	98	<i>ChemSusChem</i> 2017 , 10, 3540
Ni/Mo ₂ C-PC	0.5	GCE	368	-	<i>Chem. Sci.</i> 2017 , 8, 968
PPy/FeTCPP/Co	0.3	GCE	380	61	<i>Adv. Funct. Mater.</i> 2017 , 27, 1606497
VOOH nanospheres	0.8	Ni foam	270	68	<i>Angew. Chem. Int. Ed.</i> 2017 , 56, 573
Co ₉ S ₈ @NOSC-900	0.28	GCE	340	68	<i>Adv. Funct. Mater.</i> 2017 , 27, 1606585

Table S4. Summary of the HER and OER catalytic activities of CoP NDs, CoP ET-4, CoP ET-2 and CoP NCs.

Electrocatalyst	Reaction	η_{10} (mV)	b (mV dec ⁻¹)	Electrolyte
CoP NDs	HER	126	54.5	0.5 M H ₂ SO ₄
	HER	134	56.9	1 M KOH
	OER	318	49.1	1 M KOH
CoP ET-4	HER	142	62.8	0.5 M H ₂ SO ₄
	HER	152	64.3	1 M KOH
	OER	343	50.2	1 M KOH
CoP ET-2	HER	164	66.2	0.5 M H ₂ SO ₄
	HER	174	67.1	1 M KOH
	OER	364	59.9	1 M KOH
CoP NCs	HER	187	79.8	0.5 M H ₂ SO ₄
	HER	199	82.3	1 M KOH
	OER	388	73	1 M KOH

Table S5. Comparison of the overall water splitting activity of CoP NDs with recently reported noble-metal-free electrocatalysts in 1 M KOH.

Electrocatalyst	Loading mass (mg cm ⁻²)	Substrate	Cell voltage for 10 mA cm ⁻²	Ref.
CoP NDs	2	CC	1.62	This work
CoTeNR/NF	1.3	Ni foam	1.64	<i>Small Methods</i> 2019 , 1900113
Co ₉ S ₈ /Ni ₃ S ₂	-	Ni foam	1.64	<i>Appl. Catal. B-Environ.</i> 2019 , 253, 246
NGCs	1.5	Ni foam	1.64	<i>Carbon</i> 2019 , 150, 21
CoP@NCHNCs	1	Ni foam	1.62	<i>ACS Sustainable Chem.</i> <i>Eng.</i> 2019 , 7, 10912
NCMC	0.28	Carbon paper	1.63	<i>Chem. Commun.</i> 2019 , 55, 6515
Co-Fe oxyphosphide	-	Carbon paper	1.69	<i>Adv. Sci.</i> 2019 , 1900576
CoFe@NiFe-200/NF	-	Ni foam	1.59	<i>Appl. Catal. B-Environ.</i> 2019 , 253, 131
Ni ₃ ZnCo _{0.7} /NCNT-700	0.8	Ni foam	1.66	<i>Carbon</i> 2019 , 148, 496
Ni _{0.85} Se	2.55	Ti mesh	1.66	<i>ChemSusChem</i> 2019 , 12, 2271
NiS ₂ /CoS ₂ /C	0.2	Carbon paper	1.61	<i>Chem. Commun.</i> 2019 , 55, 3781
Co ₃ S ₄ @MoS ₂	0.6	Carbon paper	1.58	<i>Nano Energy</i> 2018 , 47, 494
hierarchical Ni-Co-P HNBS	2	Ni foam	1.62	<i>Energy Environ. Sci.</i> 2018 , 11, 872
CoP/NCNHP	2	CFP	1.64	<i>J. Am. Chem. Soc.</i> 2018 , 140, 2610
Ni/Mo ₂ C-PC	2	Ni foam	1.66	<i>Chem. Sci.</i> 2017 , 8, 968
CoTe ₂ @NCNTFs	1	Ni foam	1.67	<i>J. Mater. Chem. A</i> 2018 , 6, 3684
Mo ₂ C@CS	1	Ni foam	1.73	<i>ChemSusChem</i> 2017 , 10, 3540
CoNPs@C	3.43	CC	1.65	<i>ACS Appl. Mater.</i> <i>Interfaces</i> 2017 , 9, 31913
PPy/FeTCPP/Co	0.5	CFP	1.81	<i>Adv. Funct. Mater.</i> 2017 , 27, 1606497
CoS ₂ NTA	1.2	CC	1.67	<i>Nanoscale Horiz.</i> 2017 , 2, 342
Ni ₂ Fe ₁ -O	5.4	Ni foam	1.64	<i>Adv. Energy Mater.</i> 2018 , 8, 1701347
WO ₂ HN/NF	1.57	Ni foam	1.59	<i>J. Mater. Chem. A</i> 2017 , 5, 9655
VOOH nanospheres	0.8	Ni foam	1.62	<i>Angew. Chem. Int. Ed.</i> 2017 , 56, 573
Co ₉ S ₈ @NOSC-900	5	Ni foam	1.6	<i>Adv. Funct. Mater.</i> 2017 , 27, 1606585